Is it possible to predict ENSO frequency changes for the coming century?

F. Fix[1], **S.A. Buehler**[1], **F. Lunkeit**[1]

[1]Universität Hamburg

Key Points:

- Multi-model mean in CMIP6 1pct CO2 simulation as well as in the MPI-ESM-LR 1pct simulation predict almost no future change in ENSO frequency
- Most of the inter-model spread can be attributed to the natural variability

Corresponding author: Fiona Fix, `fiona.fix@uni-hamburg.de`

Abstract

El Niño Southern Oscillation (ENSO) is one of the most important climate variabilities on an inter-annual time-scale. We aim to find out whether ENSO frequency will change in a changing climate. We analyse two ensembles of General Circulation Models that participated in the Coupled Model Intercomparison Project Phase 6 (CMIP6) and an initial-conditions ensemble of the MPI-ESM-LR model. We identify the uncertainty caused by natural variability by comparing 120-year time-series of the pre-industrial control and the 1-percent CO_2 simulations for the CMIP6 ensembles. We found that the multi-member mean for all ensembles predicts almost no change in ENSO frequency, but the uncertainties are large, and that most of the inter-member variability can be attributed to natural variability. This means that the impact of inter-model differences might have been overstated in previous studies. This makes it impossible to make reliable predictions of changes in ENSO frequency based on 120-year simulations.

Plain Language Summary

El Niño Southern Oscillation (ENSO) is a coupled atmosphere-ocean circulation in the Pacific and of great interest since it impacts weather worldwide. The question how it will change in a changing climate is important to be able to risks due to extreme weather. Global Circulation Models can help assess this question. This study focuses on the question if ENSO frequency will change in a changing climate. We use two ensembles of 43 Global Circulation Models that participated in the Coupled Model Intercomparison Project Phase 6. By comparing the pre-industrial control simulation to a future scenario with increasing CO_2 we can identify the part of the variability caused by different behaviours of the models and the part caused by natural variability. We also use one 68-member ensemble of the MPI-ESM-LR model, because a bigger ensemble might yield statistically more reliable results. We found that on average the models predict only a very small change in ENSO frequency but the uncertainty is big. Because most of this uncertainty can be attributed to the natural variability it can be reduced only marginally. Therefore, it is impossible to make reliable predictions of changes in ENSO frequency based on 120 years of model simulations.

1 Introduction

El Niño Southern Oscillation (ENSO) is one of the most important climate variabilities on an inter-annual time-scale. Due to teleconnections it impacts weather conditions worldwide and can lead to extreme weather events. To reduce the social, economic and environmental risk of theses events, accurate forecasting is required. Therefore, understanding and predicting ENSO mechanisms is a central question of current research. In particular, the question of how ENSO will react to global warming is of great interest. Global warming could have different effects on the equatorial Pacific and therefore on ENSO. ENSO frequency can be affected by the strength and depth of the equatorial thermocline, the meridional and zonal sea surface temperature (SST) gradients as well as the strength of the trade winds (Yang et al., 2005; Deng et al., 2010). How these (and other) mechanisms work together and which one(s) will predominate, defines how ENSO will react in future and has yet to be investigated. If and how ENSO behaviour will change under a changing climate has been studied intensely in the past years.

Some studies found an increase in ENSO frequency in the models they examined (Timmermann et al., 1999; Collins, 2000a). Collins (2000a) for example studied ENSO frequency with the second Hadley Centre coupled climate model (HadCM2). The HadCM2 is a coupled climate model which, according to Collins (2000a), represents present day ENSO conditions (amplitude and frequency) well. When running different climate change scenarios he finds that there are only small changes until a quadrupling of CO_2, when the frequency doubles. On the other hand Yang et al. (2005) investigated ENSO in the

Fast Ocean-Atmosphere Model and find that a reduction of ENSO frequency is very likely as a result of warming climate. Yet other studies argue that ENSO frequency does not react to global warming at all (e.g. Timmermann, 2001; Zelle et al., 2005). Also, Collins (2000b) follows up on his earlier study and finds that in the third Hadley Centre coupled climate model (HadCM3) there is no change to ENSO frequency under different climate change scenarios. Both Zelle et al. (2005) and Collins (2000b) emphasise the effect that model specifics can have on the sensitivity of ENSO to climate change. Therefore, to increase the robustness multi-model ensembles have been used in many later studies. In a study by Merryfield (2006) 12 out of 15 models (prepared for IPCC AR4) agreed on a decrease in ENSO period. Cai et al. (2014); Cai, Santoso, et al. (2015) and Cai, Wang, et al. (2015) analysed models participating in the Coupled Model Intercomparison Project, Phases 3 and 5. They conclude, that there is a high inter model agreement, that extreme El Niño/ La Niña events become more frequent in a warming climate. Wang et al. (2017) also use 13 models participating in Coupled Model Intercomparison Project Phase 5 (CMIP5) and come to the same conclusion. But, many studies that have investigated multi-model ensembles come to the conclusion that the predictions of ENSO frequency are strongly model dependent. Studies by Guilyardi (2006), Deng et al. (2010), Xu et al. (2017) and Chen et al. (2017) suggest that the model consensus is very small on the topic of how ENSO frequency will change in a changing climate.

Chen et al. (2017) mention that the difficulty in predicting ENSO properties is not only the inter-model spread but also the significant natural variability and Zheng et al. (2018) support this hypothesis in a study about ENSO amplitude. A similar study by Maher et al. (2018) shows that (depending on the warming scenario) up to 90% of the variability of ENSO amplitude can be attributed to internal variability. In this study we want to quantify the aspect of natural variability of ENSO frequency. Climate forecasts can be improved by using multi-model ensembles (Xu et al., 2017) instead of single simulations because parametrisation errors of individual models are expected to be averaged out. The uncertainty due to differences in the model realisation is reducible but it is not the only uncertainty in such ensembles. The chaotic nature of the climate system will cause an internal variability which remains irreducible. We want to identify the signal caused by this internal climate variability. Therefore we make use of the multi-model ensemble that is part of the Coupled Model Intercomparison Project Phase 6 (CMIP6). We compare the simulation with increased CO_2 to the pre-industrial control simulation. By doing so we can estimate how much of the variability is caused by the different model responses to the forcing and how much is due to internal variability.

Additional to the multi-model ensemble we analyse a bigger ensemble resulting from running the MPI-ESM-LR model with perturbed initial conditions, to increase the statistical confidence of our results. As suggested by Maher et al. (2018), the use of large single-model ensembles can give important insight into changes in ENSO properties.

2 Data

In this work we first make use of two multi-model ensembles of CMIP6, which consist of 43 members (a list with detailed information can be found in table 1). We compare the simulations for the 1 percent CO_2 (1pct CO2) experiment to the pre-industrial Control (piControl) simulations. In the piControl experiment 1850 is used as a reference year and the simulations are run for at least 500 years (Eyring et al., 2016). The 1pct CO2 simulation is initialised from the control run. A 150-year period is simulated during which the CO_2 concentration is continuously increased by 1% per year. This results in a doubling of CO_2 after 70 and a quadrupling after 140 years, respectively (Giorgetta et al., 2013). To make the two ensembles comparable we only use the last 150 years of the piControl run. For the IPSL model apparently files were added at different times. Because the files' meta-data implied that the later simulations might not actually be from the same model version and the first simulation is already 500 years long, we decided to

Table 1. List of the 43 CMIP6 models used in this study.

No.	Model	Variant	Version	1pct	pi Control	Institute	Resolution[a] ocean, latxlon	Reference
1	ACCESS-CSM2	r1i1p1f1	v20191109	x		CSIRO	300x360	Dix et al. (2019)
			v20191112		x			
2	ACCESS-ESM1-5	r1i1p1f1	v201911115	x		CSIRO	300x360	Ziehn et al. (2019)
			v20191214[b]		x			
3	AWI-CM-1-1-MR	r1i1p1f1	v20181218	x	x	AWI	83030[c]	Semmler et al. (2018)
4	BCC-CSM2-MR	r1i1p1f1	v20181015	x	x	BCC	232x360	Xin et al. (2018)
5	BCC-ESM1	r1i1p1f1	v20190611	x		BCC	232x360	Zhang et al. (2018)
			v20181218		x			
6	CAMS-CSM1-0	r1i1p1f1	v20190708[b]	x		CAMS	200x360	Rong (2019)
			v20190729[b]		x			
7	CESM-FV2	r1i1p1f1	v20200310[b]	x		NCAR	384x320	Danabasoglu (2019a)
			v20191120[b]		x			
8	CESM-WACCM-FV2	r1i1p1f1	v20200226[b]	x		NCAR	384x320	Danabasoglu (2019c)
			v20191120[b]		x			
9	CESM2-WACCM	r1i1p1f1	v20190425[b]	x		NCAR	384x320	Danabasoglu (2019d)
			v20190320[b]		x			
10	CESM2	r1i1p1f1	v20190425[b]	x		NCAR	384x320	Danabasoglu (2019b)
			v20190320[b]		x			
11	CIESM	r1i1p1f1	v20200220[b]	x	x	THU	384x320	Huang (2019)
12	CNRM-CM6-1-HR	r1i1p1f2	v20191021[b]	x	x	CNRM-CERFACS	1050x1442	Voldoire (2019)
13	CNRM-CM6-1	r1i1p1f2	v20180626[b]	x		CNRM-CERFACS	294x362	Voldoire (2018)
			v20180814[b]		x			
14	CNRM-ESM2-1	r1i1p1f2	v20181018[b]	x		CNRM-CERFACS	294x362	Seferian (2018)
			v29181115[b]		x			
15	CanESM5	r1i1p1f1	v20190429	x	x	CCCma	291x360	Swart et al. (2019)
16	CanESM5	r1i1p2f1	v20190429	x	x	CCCma	291x360	Swart et al. (2019)
17	E3SM-1-0	r1i1p1f1	v20191008	x		E3SM-Project	180x360	Bader et al. (2019)
			v20200129[b]		x			
18	EC-Earth3	r3i1p1f1	v20200727[b]	x		EC-Earth-Consortium	292x362	EC-Earth Consortium (2019)
		r2i1p1f1	v20200420[b]		x			
19	FIO-ESM-2-0	r1i1p1f1	v20200306	x		FIO-QLNM	384x320	Song et al. (2019)
			v20191012		x			
20	GFDL-CM4	r1i1p1f1	v20180701	x		NOAA-GFDL	1080x1440	Guo et al. (2018)
			v20190201		x			
21	GISS-E2-1-G	r102i1p1f1	v20190815	x	x	NASA-GISS	90x144	NASA/GISS (2018a)
22	GISS-E2-1-G	r1i1p1f1	v20190824	x	x	NASA-GISS	90x144	NASA/GISS (2018a)
23	GISS-E2-1-G	r1i1p5f1	v20190905	x		NASA-GISS	90x144	NASA/GISS (2018a)
			v20190710		x			
24	GISS-E2-1-H	r1i1p1f1	v20190403[b]	x		NASA-GISS	90x144	NASA/GISS (2018b)
			v20190410[b]		x			
25	GISS-E2-2-G	r1i1p1f1	v20191120[b]	x	x	NASA-GISS	90x144	NASA/GISS (2019)
26	HadGEM3-GC31-LL	r1i1p1f3	v20190620[b]	x		MOHC	330x360	Ridley et al. (2018)
		r1i1p1f1	v20190628[b]		x			
27	INM-CM4-8	r1i1p1f1	v20190530	x		INM	180x360	Volodin et al. (2019a)
			v20190605[b]		x			
28	INM-CM5-0	r1i1p1f1	v20200226	x		INM	180x360	Volodin et al. (2019b)
			v20190619		x			
29	IPSL-CM6A-LR	r1i1p1f1	v20180727	x		IPSL	332x362	Boucher et al. (2018)
			v20200326		x			
30	MCM-UA-1-0	r1i1p1f1	v20190731	x	x	UA	80x192	Stouffer (2019)
31	MIROC-ES2L	r1i1p1f2	v20190823	x	x	MIROC	256x360	Hajima et al. (2019)
32	MIROC6	r1i1p1f1	v20181212	x	x	MIROC	256x360	Tatebe and Watanabe (2018)
33	MPI-ESM-1-2-HAM	r1i1p1f1	v20190628	x		HAMMOZ-Consortium	220x256	Neubauer et al. (2019)
			v20190627		x			
34	MPI-ESM1-2-HR	r1i1p1f1	v20190710	x	x	MPI-M	404x802	Jungclaus et al. (2019)
35	MPI-ESM1-2-LR	r1i1p1f1	v20190710	x	x	MPI-M	220x256	Wieners et al. (2019)
36	MRI-ESM2-0	r1i1p1f1	v20190904[b]	x	x	MRI	363x360	Yukimoto et al. (2019)
37	MRI-ESM2-0	r1i2p1f1	v20200303 [b]	x		MRI	363x360	Yukimoto et al. (2019)
			v20200222[b]		x			
38	NESM3	r1i1p1f1	v20190703	x		NUIST	292x362	Cao and Wang (2019)
			v20190704		x			
39	NorCPM1	r1i1p1f1	v20190914	x	x	NCC	384x320	Bethke et al. (2019)
40	NorESM2-LM	r1i1p1f1	v20190815	x		NCC	385x360	Seland et al. (2019)
			v20210118[b]		x			
41	NorESM2-MM	r1i1p1f1	v20191108	x	x	NCC	385x360	Bentsen et al. (2019)
42	SAM0-UNICON	r1i1p1f1	v20190323	x		SNU	384x320	Park and Shin (2019)
			v20190910		x			
43	UKESM1-0-LL	r1i1p1f2	v20190701	x		MOHC	330x360	Tang et al. (2019)
			v20200828		x			

[a] Some files have different resolution information in the meta-data .
We use the resolution that can be determined from the size of the variable-array
[b] For these files the creation date precedes the date according to the version number.
We nevertheless assume that the version number date is correct.
[c] Irregular grid, number of grid points

use the last 150 years of this first simulation instead of the later ones. The ensembles will be referred to as 1pct- and Control-ensemble, respectively.

Another ensemble used in this study is an initial-conditions ensemble. The MPI-ESM-LR model has been run for the 1pctCO2 experiment with slightly different initial conditions which results in a 68-member ensemble (Plesca et al., 2018; Giorgetta et al., 2013; Stevens et al., 2013). This ensemble will from now on be referred to as MPI-ensemble. It should be mentioned that this ensemble is older than the CMIP6 ones, since it was run for the CMIP5. The reason for using an older ensemble for this work was the availability of this dataset.

3 Methods

There are many indices to measure ENSO activity, which all have their advantages and disadvantages. Depending on the available data and the question posed, different indices prove to be helpful. In this work we make use of an index based on the first empirical orthogonal function (EOF) of SST data from the tropical Pacific (120°E-60°W, 30°N-30°S). The pattern of the first EOF explains most of the variability in the tropical Pacific, particularly in the Nino3.4 region (Dommenget et al., 2013). Therefore, the principle component (PC) of the first EOF can be used as an ENSO-index (a very similar approach was used in other studies (e.g. Merryfield, 2006; Berner et al., 2020)). In fact, it can be shown that this index is highly correlated with the Ocean Nino Index (ONI) defined by NOAA Climate Prediction Center, National Weather Service (2020a) (Berner et al., 2020; Penland & Sardeshmukh, 1995). This means that they indeed describe the same ENSO variations. We calculated the correlation between these two indices for the 43-member ensemble of the CMIP6 piControl experiment and obtained a mean value of 0.971 (min: 0.883, max: 0.991).

In order to calculate this index the climate trend and annual cycle have to be eliminated. This is done as described by NOAA Climate Prediction Center, National Weather Service (2020a) for the ONI. Anomalies are calculated for each grid-point with respect to a centred base-period. This base-period is updated every 5 years to account for the warming trend in the region. The base-period corresponding to the years x to x+5 is the period x-15 to x+15 (NOAA Climate Prediction Center, National Weather Service, 2020b). Subsequently, the anomalies are smoothed by a 3-month-running mean. From these smoothed anomalies EOFs can be calculated, which also yields the time series of the PCs. The first PC is used as the ENSO-index in this study and will be referred to as the PC-index. The base-period-method creates artificial trends at the beginning and end of a dataset, because for the first and last 15 years there is no centred base-period available. Therefore, the first base-period has to be used for the first 20 years and the last base-period for the last 20 years. This creates an unwanted effect, which can't be corrected. Therefore the first and last 15 years of data can not be correctly evaluated and will not be taken into account for further analysis. We therefore effectively analyse time series with a length of 120 years.

According to the NOAA Climate Prediction Center, National Weather Service (2020a) conditions are considered "El Niño-like" when the ONI exceeds +0.5 K and "La Niña-like" when the index goes below -0.5 K. Whenever conditions are met for 5 consecutive months, it is called an "El Niño event" or a "La Niña event". We use the same definition for the PC-index as well.

Similarly to Deng et al. (2010) we count El Niño and La Niña events to estimate changes in ENSO frequency. In this study we use a 30-year moving window. The number of months within a 30-year period that were "El Niño-" or "La Niña-like" were counted as well as the number of actual El Niño or La Niña events within this period. This results in a time series of occurrences, of which a linear regression can be calculated. The slope of this regression line defines the linear trend in the amount of "El Niño-" and "La Niña-like" months and -events. It provides insight into how the number of El Niño/La Niña events will increase or decrease over the years. We have computed the linear trend

Table 2. Means and standard deviations σ of predicted changes in occurrences of El Niño (EN) and La Niña (LN) events and "EN/LN-like" conditions for all three ensembles[a].

	EN		LN		"EN-like"		"LN-like"	
ensemble	mean	σ	mean	σ	mean	σ	mean	σ
1pct	0.038 ± 0.038	0.2506	0.108 ± 0.030	0.1987	0.094 ± 0.441	2.8919	0.622 ± 0.444	2.9101
Control	-0.040 ± 0.032	0.2085	0.022 ± 0.040	0.2615	-0.290 ± 0.386	2.5319	0.179 ± 0.412	2.7047
MPI	0.070 ± 0.030	0.2514	0.020 ± 0.029	0.2364	-0.169 ± 0.374	3.0849	-0.320 ± 0.390	3.2138

[a] All numbers are unitless, they represent changes in occurences during one decade.

for every member of each of the three ensembles. For convenience, the gradient in months^{-1} can be converted into a more intuitive measure for the change in ENSO frequency by multiplying it by 120 months, which then gives the change in the number of occurrences during a decade.

4 Results

Figures 1 and 2 show the linear trend of El Niño and La Niña -events and -like months. On average the 1pct-ensemble predicts an increase of 0.038 ± 0.038 El Niño events and an increase of 0.108 ± 0.030 La Niña events per decade (the ± values are the standard errors, $\sigma/\sqrt{N}$). The standard deviations (σ) are 0.2506 and 0.1987 events per decade for El Niño and La Niña events, respectively. Hence, the inter-model spread appears to be larger than the mean change itself, which makes it difficult to detect changes in ENSO frequency (see Tab. 2).

An interesting question is whether this uncertainty can be reduced at all. Therefore we compare the 1pct-ensemble to the Control-ensemble. It can be expected that the 1pct-ensemble contains uncertainties (σ_{1pct}) due to the different reactions of the different models to the forcing ($\sigma_{\mathrm{ModelDiff}}$) as well as uncertainties due to the natural variability ($\sigma_{\mathrm{NaturalVariability}}$). Under the assumption that the errors are uncorrelated this results in

$$\sigma^2_{\mathrm{1pct}} = \sigma^2_{\mathrm{ModelDiff}} + \sigma^2_{\mathrm{NaturalVariability}} \quad (1)$$

Therefore its standard deviation should be greater than the standard deviation of the Control-ensemble, which only contains the uncertainty due to natural variability:

$$\sigma^2_{\mathrm{Control}} = \sigma^2_{\mathrm{NaturalVariability}} \quad (2)$$

Still under the assumption of uncorrelated errors, the difference in the variances σ^2 of the two ensembles should be a measure for the uncertainty caused by model differences, ie.

$$\sigma^2_{\mathrm{ModelDiff}} = \sigma^2_{\mathrm{1pct}} - \sigma^2_{\mathrm{Control}} \quad (3)$$

This uncertainty can be reduced, while the rest, the natural variability, will remain.

For El Niño events the standard deviation due to model differences is therefore 0.1369 events per decade, which is one order of magnitude less than the standard deviation due to natural variability. For La Niña events the difference in variances is even negative with -0.0281.

This means that the biggest part of the uncertainty in the 1pct-ensemble prediction stems from the natural variability and is therefore irreducible, since the real world

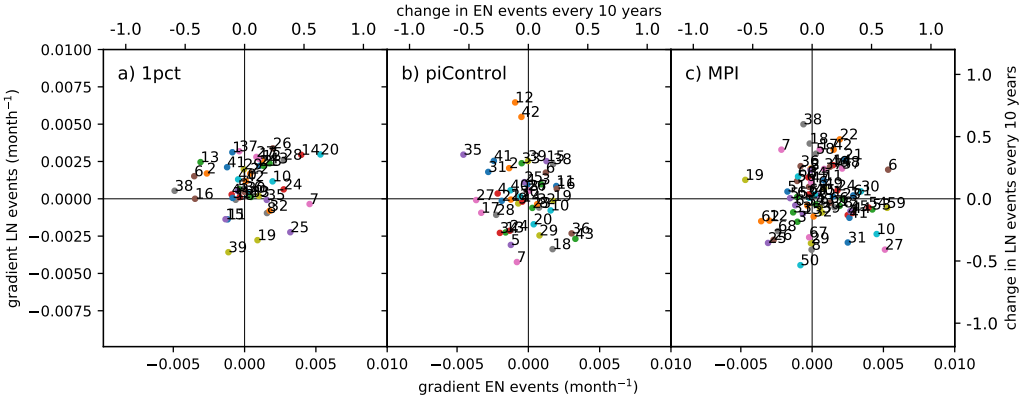

Figure 1. Linear Trend in El Niño/La Niña events for each member of the three ensembles: a) the 1pct-ensemble, b) the Control-ensemble, c) the MPI-ensemble. Values towards the top of the plot indicate increasing number of La Niña (LN) events, values toward the right of the plot indicate an increasing number of El Niño (EN) events. Numbers in panels a) and b) correspond to models as in table 1.

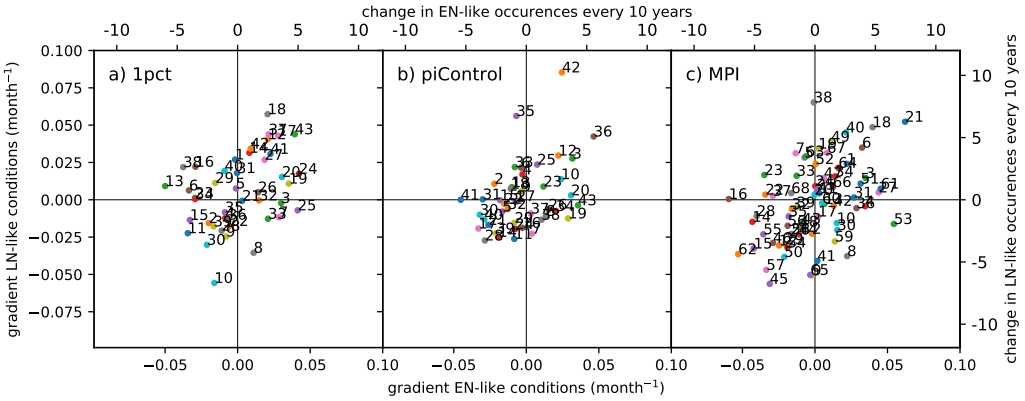

Figure 2. Same as figure 1 but for "El Niño-" and "La Niña-like" conditions.

will evolve like one ensemble member, not like the ensemble mean. Since the uncertainty is in the range of the predicted mean changes or even exceeds them, no reliable forecast can be made on the time-scale of 120 years. The result is qualitatively the same for the "El Niño-" and "La Niña-like" conditions (see Tab. 2 and Fig. 2)

A statistically more reliable result might be achieved by analysing a bigger ensemble. Therefore we conducted the same analysis for the MPI-ensemble, which consists of 68 members. The MPI-ESM-LR model was run with perturbed initial conditions for the 1pct CO2 experiment in CMIP5. Since it is an initial-conditions ensemble it only contains the uncertainty due to natural variability. For the change in El Niño events the bigger ensemble predicts a change of 0.069 $\pm$ 0.030 events per decade. The uncertainty seems to be slightly less compared to the earlier analysis. But for the La Niña events and the "El Niño-" and "La Niña-like" conditions the uncertainty is of the same order of magnitude or bigger than the expected change itself again. This supports the assumption that a reliable prediction of ENSO-frequency on a time-scale of 120 years cannot be made.

5 Discussion and Conclusions

The multi-model mean frequency change of El Niño and La Niña events is less than ± 0.2 events per decade in all three ensembles and in all cases the uncertainties are large. Our analysis of the two CMIP6 ensembles showed that the natural variability dominates the results. This suggests that the stronger trends found in individual models like in the studies by Timmermann et al. (1999) or Yang et al. (2005) may be mostly due to natural variability. Also the results from Timmermann (2001) and Zelle et al. (2005) who found no trend in the respective models therefore have to be treated carefully. In contrast to the studies by Merryfield (2006), Cai et al. (2014), Cai, Wang, et al. (2015), Cai, Santoso, et al. (2015) and Wang et al. (2017) we could not find an inter-model consensus on a significant trend in ENSO frequency in the ensembles. It should be mentioned though, that we did not distinguish between normal and extreme El Niño and La Niña events like some of the mentioned authors did.

Zelle et al. (2005) and Collins (2000b) suggested that prediction of ENSO frequency is strongly model dependent and the studies by Guilyardi (2006), Deng et al. (2010), Xu et al. (2017) and Chen et al. (2017) indeed found a poor inter-model consensus. Our study implies though that it is actually not the model differences that are responsible for the biggest part of the inter-model spread but rather the natural variability. This does not mean that model differences do not play a role, only that their importance relative to natural variability likely has been overstated. We therefore complement the findings of Chen et al. (2017), who found that for changes in for example ENSO asymmetry in amplitude, duration, and transition from the 20th to the 21st century the model agreement is poor, trends are not significant and the variations mostly lie within the range of natural variability. Our findings also support the results from the studies by Zheng et al. (2018) and Maher et al. (2018) who did similar analyses but for ENSO amplitude and also attribute most inter-member variability to natural variability.

Our results suggest that the uncertainties might only be marginally reducible, since only the uncertainties due to model differences can be minimised but not the natural variability. This means that it is impossible to make reliable predictions of changes in ENSO frequency based on 120 years of model simulations. Although we used only a particular type of model (coupled climate models as represented in CMIP) we think that this result is general, since the main finding is that the natural variability is so large, and this is unlikely to change for more sophisticated models. Therefore, even if models that represent ENSO dynamics more faithfully may exhibit larger and/or more robust ENSO frequency trends, natural variability is still likely to dominate.

Acronyms

CMIP5 Coupled Model Intercomparison Project Phase 5
CMIP6 Coupled Model Intercomparison Project Phase 6
ENSO El Niño Southern Oscillation
EOF empirical orthogonal function
PC principle component
SST sea surface temperature

Acknowledgments
We thank the WorldClimate Research Programme's Working Group on Coupled Modelling who are responsible for CMIP6, for making the datasets used in this study publicly available. Special thanks to the modelling groups and institutes that responsible for the models listed in table 1. All CMIP6 data used in this work is made available by the DKRZ (Deutsches Klimarechenzentrum). We also want to send special thanks to the

Max-Planck Institute for Meteorology in Hamburg for providing the MPI-ESM-LR simulations.

Thanks to Thorsten Mauritsen for the idea to look at the control runs. Thanks also go to Oliver Lemke for any kind of technical support.

With this study we contribute to the Center for Earth System Research and Sustainability (CEN) of Universität Hamburg. The work of Fiona Fix was supported by the Deutsche Forschungsgemeinschaft (DFG, German Research Foundation) under Germany's Excellence Strategy – EXC 2037 'CLICCS - Climate, Climatic Change, and Society' – Project Number: 390683824.

References

Bader, D. C., Leung, R., Taylor, M., & McCoy, R. B. (2019). *E3SM-Project E3SM1.0 model output prepared for CMIP6 CMIP.* Earth System Grid Federation. Retrieved from https://doi.org/10.22033/ESGF/CMIP6.2294 doi: 10.22033/ESGF/CMIP6.2294

Bentsen, M., Oliviè, D. J. L., Seland, y., Toniazzo, T., Gjermundsen, A., Graff, L. S., ... Schulz, M. (2019). *NCC NorESM2-MM model output prepared for CMIP6 CMIP.* Earth System Grid Federation. Retrieved from https://doi.org/10.22033/ESGF/CMIP6.506 doi: 10.22033/ESGF/CMIP6.506

Berner, J., Christensen, H. M., & Sardeshmukh, P. D. (2020). Does ENSO Regularity Increase in a Warming Climate? *Journal of Climate*, *33*(4), 1247-1259. Retrieved from https://doi.org/10.1175/JCLI-D-19-0545.1 doi: 10.1175/JCLI-D-19-0545.1

Bethke, I., Wang, Y., Counillon, F., Kimmritz, M., Fransner, F., Samuelsen, A., ... Keenlyside, N. (2019). *NCC NorCPM1 model output prepared for CMIP6 CMIP.* Earth System Grid Federation. Retrieved from https://doi.org/10.22033/ESGF/CMIP6.10843 doi: 10.22033/ESGF/CMIP6.10843

Boucher, O., Denvil, S., Levavasseur, G., Cozic, A., Caubel, A., Foujols, M.-A., ... Cheruy, F. (2018). *IPSL IPSL-CM6A-LR model output prepared for CMIP6 CMIP.* Earth System Grid Federation. Retrieved from https://doi.org/10.22033/ESGF/CMIP6.1534 doi: 10.22033/ESGF/CMIP6.1534

Cai, W., Borlace, S., Lengaigne, M., Rensch, P., Collins, M., Vecchi, G., ... Jin, F.-F. (2014). Increasing Frequency of Extreme El Nino Events due to Greenhouse Warming. *Nature Climate Change*, *4*, 111–116. Retrieved from https://doi.org/10.1038/nclimate2100 doi: 10.1038/nclimate2100

Cai, W., Santoso, A., Wang, G., Yeh, S.-W., An, S.-I., Cobb, K. M., ... Wu, L. (2015). ENSO and greenhouse warming. *Nature Climate Change*, *5*, 849-859. Retrieved from https://doi.org/10.1038/nclimate2743 doi: 10.1038/nclimate2743

Cai, W., Wang, G., Santoso, A., McPhaden, M., Wu, L., Jin, F.-F., ... Guilyardi, E. (2015). Increased frequency of extreme La Niña events under greenhouse warming. *Nature Climate Change*, *5*, 132-137. Retrieved from https://doi.org/10.1038/nclimate2492 doi: 10.1038/nclimate2492

Cao, J., & Wang, B. (2019). *NUIST NESMv3 model output prepared for CMIP6 CMIP.* Earth System Grid Federation. Retrieved from https://doi.org/10.22033/ESGF/CMIP6.2021 doi: 10.22033/ESGF/CMIP6.2021

Chen, C., Cane, M. A., Wittenberg, A. T., & Chen, D. (2017). ENSO in the CMIP5 Simulations: Life Cycles, Diversity, and Responses to Climate Change. *Journal of Climate*, *30*(2), 775 - 801. Retrieved from https://journals.ametsoc.org/view/journals/clim/30/2/jcli-d-15-0901.1.xml doi: 10.1175/JCLI-D-15-0901.1

Collins, M. (2000a). The el niño–southern oscillation in the second hadley centre coupled model and its response to greenhouse warming. *Journal of Climate*,

13(7), 1299 - 1312. Retrieved from https://journals.ametsoc.org/view/journals/clim/13/7/1520-0442_2000_013_1299_tenoso_2.0.co_2.xml doi: 10.1175/1520-0442(2000)013⟨1299:TENOSO⟩2.0.CO;2

Collins, M. (2000b). Understanding uncertainties in the response of ENSO to greenhouse warming. *Geophysical Research Letters*, *27*(21), 3509-3512. Retrieved from https://agupubs.onlinelibrary.wiley.com/doi/abs/10.1029/2000GL011747 doi: https://doi.org/10.1029/2000GL011747

Danabasoglu, G. (2019a). *NCAR CESM2-FV2 model output prepared for CMIP6 CMIP.* Earth System Grid Federation. Retrieved from https://doi.org/10.22033/ESGF/CMIP6.11281 doi: 10.22033/ESGF/CMIP6.11281

Danabasoglu, G. (2019b). *NCAR CESM2 model output prepared for CMIP6 CMIP.* Earth System Grid Federation. Retrieved from https://doi.org/10.22033/ESGF/CMIP6.2185 doi: 10.22033/ESGF/CMIP6.2185

Danabasoglu, G. (2019c). *NCAR CESM2-WACCM-FV2 model output prepared for CMIP6 CMIP.* Earth System Grid Federation. Retrieved from https://doi.org/10.22033/ESGF/CMIP6.11282 doi: 10.22033/ESGF/CMIP6.11282

Danabasoglu, G. (2019d). *NCAR CESM2-WACCM model output prepared for CMIP6 CMIP.* Earth System Grid Federation. Retrieved from https://doi.org/10.22033/ESGF/CMIP6.10024 doi: 10.22033/ESGF/CMIP6.10024

Deng, L., Yang, X., & Xie, Q. (2010). ENSO frequency change in coupled climate models as response to the increasing CO_2 concentration. *Chinese Science Bulletin*, *55*, 744-751. Retrieved from https://doi.org/10.1007/s11434-009-0491-x doi: 10.1007/s11434-009-0491-x

Dix, M., Bi, D., Dobrohotoff, P., Fiedler, R., Harman, I., Law, R., ... Yang, R. (2019). *CSIRO-ARCCSS ACCESS-CM2 model output prepared for CMIP6 CMIP.* Earth System Grid Federation. Retrieved from https://doi.org/10.22033/ESGF/CMIP6.2281 doi: 10.22033/ESGF/CMIP6.2281

Dommenget, D., Bayr, T., & Frauen, C. (2013). Analysis of the non-linearity in the pattern and time evolution of El Niño southern oscillation. *Climate Dynamics*, *40*, 2825–2847. Retrieved from https://doi.org/10.1007/s00382-012-1475-0 doi: 10.1007/s00382-012-1475-0

EC-Earth Consortium. (2019). *EC-Earth-Consortium EC-Earth3 model output prepared for CMIP6 CMIP.* Earth System Grid Federation. Retrieved from https://doi.org/10.22033/ESGF/CMIP6.181 doi: 10.22033/ESGF/CMIP6.181

Eyring, V., Bony, S., Meehl, G. A., Senior, C. A., Stevens, B., Stouffer, R. J., & Taylor, K. E. (2016). Overview of the Coupled Model Intercomparison Project Phase 6 (CMIP6) experimental design and organization. *Geoscientific Model Development*, *9*(5), 1937–1958. Retrieved from https://gmd.copernicus.org/articles/9/1937/2016/ doi: 10.5194/gmd-9-1937-2016

Giorgetta, M. A., Jungclaus, J., Reick, C. H., Legutke, S., Bader, J., Böttinger, M., ... Stevens, B. (2013). Climate and carbon cycle changes from 1850 to 2100 in MPI-ESM simulations for the Coupled Model Intercomparison Project phase 5. *Journal of Advances in Modeling Earth Systems*, *5*(3), 572-597. Retrieved from https://agupubs.onlinelibrary.wiley.com/doi/abs/10.1002/jame.20038 doi: 10.1002/jame.20038

Guilyardi, E. (2006). El Niño–mean state–seasonal cycle interactions in a multi-model ensemble. *Climate Dynamics*, *26*, 329-348. Retrieved from https://doi.org/10.1007/s00382-005-0084-6 doi: 10.1007/s00382-005-0084-6

Guo, H., John, J. G., Blanton, C., McHugh, C., Nikonov, S., Radhakrishnan, A., ... Zhang, R. (2018). *NOAA-GFDL GFDL-CM4 model output.* Earth System Grid Federation. Retrieved from https://doi.org/10.22033/ESGF/CMIP6.1402 doi: 10.22033/ESGF/CMIP6.1402

Hajima, T., Abe, M., Arakawa, O., Suzuki, T., Komuro, Y., Ogura, T., ... Tachiiri, K. (2019). *MIROC MIROC-ES2L model output prepared for CMIP6 CMIP.*

Earth System Grid Federation. Retrieved from https://doi.org/10.22033/ESGF/CMIP6.902 doi: 10.22033/ESGF/CMIP6.902

Huang, W. (2019). *THU CIESM model output prepared for CMIP6 CMIP.* Earth System Grid Federation. Retrieved from https://doi.org/10.22033/ESGF/CMIP6.1352 doi: 10.22033/ESGF/CMIP6.1352

Jungclaus, J., Bittner, M., Wieners, K.-H., Wachsmann, F., Schupfner, M., Legutke, S., ... Roeckner, E. (2019). *MPI-M MPIESM1.2-HR model output prepared for CMIP6 CMIP.* Earth System Grid Federation. Retrieved from https://doi.org/10.22033/ESGF/CMIP6.741 doi: 10.22033/ESGF/CMIP6.741

Maher, N., Matei, D., Milinski, S., & Marotzke, J. (2018). ENSO Change in Climate Projections: Forced Response or Internal Variability? *Geophysical Research Letters*, *45*(20), 11,390-11,398. Retrieved from https://agupubs.onlinelibrary.wiley.com/doi/abs/10.1029/2018GL079764 doi: https://doi.org/10.1029/2018GL079764

Merryfield, W. J. (2006). Changes to ENSO under CO2 Doubling in a Multimodel Ensemble. *Journal of Climate*, *19*(16), 4009 - 4027. Retrieved from https://journals.ametsoc.org/view/journals/clim/19/16/jcli3834.1.xml doi: 10.1175/JCLI3834.1

NASA/GISS. (2018a). *NASA-GISS GISS-E2.1G model output prepared for CMIP6 CMIP.* Earth System Grid Federation. Retrieved from https://doi.org/10.22033/ESGF/CMIP6.1400 doi: 10.22033/ESGF/CMIP6.1400

NASA/GISS. (2018b). *NASA-GISS GISS-E2.1H model output prepared for CMIP6 CMIP.* Earth System Grid Federation. Retrieved from https://doi.org/10.22033/ESGF/CMIP6.1421 doi: 10.22033/ESGF/CMIP6.1421

NASA/GISS. (2019). *NASA-GISS GISS-E2-2-G model output prepared for CMIP6 CMIP.* Earth System Grid Federation. Retrieved from https://doi.org/10.22033/ESGF/CMIP6.2081 doi: 10.22033/ESGF/CMIP6.2081

Neubauer, D., Ferrachat, S., Siegenthaler-Le Drian, C., Stoll, J., Folini, D. S., Tegen, I., ... Lohmann, U. (2019). *HAMMOZ-Consortium MPI-ESM1.2-HAM model output prepared for CMIP6 CMIP.* Earth System Grid Federation. Retrieved from https://doi.org/10.22033/ESGF/CMIP6.1622 doi: 10.22033/ESGF/CMIP6.1622

NOAA Climate Prediction Center, National Weather Service. (2020a). *Cold & Warm Episodes by Season.* Retrieved from https://origin.cpc.ncep.noaa.gov/products/analysis_monitoring/ensostuff/ONI_v5.php (Online, last accessed 22-March-2021)

NOAA Climate Prediction Center, National Weather Service. (2020b). *Description of Changes to Ocean Niño Index (ONI).* Retrieved from https://origin.cpc.ncep.noaa.gov/products/analysis_monitoring/ensostuff/ONI_change.shtml (Online, last accessed 22-March-2021)

Park, S., & Shin, J. (2019). *SNU SAM0-UNICON model output prepared for CMIP6 CMIP.* Earth System Grid Federation. Retrieved from https://doi.org/10.22033/ESGF/CMIP6.1489 doi: 10.22033/ESGF/CMIP6.1489

Penland, C., & Sardeshmukh, P. D. (1995). The Optimal Growth of Tropical Sea Surface Temperature Anomalies. *Journal of Climate*, *8*(8), 1999-2024. Retrieved from https://doi.org/10.1175/1520-0442(1995)008<1999:TOGOTS>2.0.CO;2 doi: 10.1175/1520-0442(1995)008⟨1999:TOGOTS⟩2.0.CO;2

Plesca, E., Grützun, V., & Buehler, S. A. (2018). How robust is the weakening of the pacific walker circulation in cmip5 idealized transient climate simulations? *Journal of Climate*, *31*(1), 81 - 97. Retrieved from https://journals.ametsoc.org/view/journals/clim/31/1/jcli-d-17-0151.1.xml doi: 10.1175/JCLI-D-17-0151.1

Ridley, J., Menary, M., Kuhlbrodt, T., Andrews, M., & Andrews, T. (2018). *MOHC HadGEM3-GC31-LL model output prepared for CMIP6 CMIP.* Earth System Grid Federation. Retrieved from https://doi.org/10.22033/ESGF/

CMIP6.419 doi: 10.22033/ESGF/CMIP6.419

Rong, X. (2019). *CAMS CAMS_CSM1.0 model output prepared for CMIP6 CMIP.* Earth System Grid Federation. Retrieved from https://doi.org/10.22033/ESGF/CMIP6.1399 doi: 10.22033/ESGF/CMIP6.1399

Seferian, R. (2018). *CNRM-CERFACS CNRM-ESM2-1 model output prepared for CMIP6 CMIP.* Earth System Grid Federation. Retrieved from https://doi.org/10.22033/ESGF/CMIP6.1391 doi: 10.22033/ESGF/CMIP6.1391

Seland, y., Bentsen, M., Oliviè, D. J. L., Toniazzo, T., Gjermundsen, A., Graff, L. S., ... Schulz, M. (2019). *NCC NorESM2-LM model output prepared for CMIP6 CMIP.* Earth System Grid Federation. Retrieved from https://doi.org/10.22033/ESGF/CMIP6.502 doi: 10.22033/ESGF/CMIP6.502

Semmler, T., Danilov, S., Rackow, T., Sidorenko, D., Barbi, D., Hegewald, J., ... Jung, T. (2018). *AWI AWI-CM1.1MR model output prepared for CMIP6 CMIP.* Earth System Grid Federation. Retrieved from https://doi.org/10.22033/ESGF/CMIP6.359 doi: 10.22033/ESGF/CMIP6.359

Song, Z., Qiao, F., Bao, Y., Shu, Q., Song, Y., & Yang, X. (2019). *FIO-QLNM FIO-ESM2.0 model output prepared for CMIP6 CMIP.* Earth System Grid Federation. Retrieved from https://doi.org/10.22033/ESGF/CMIP6.9047 doi: 10.22033/ESGF/CMIP6.9047

Stevens, B., Giorgetta, M., Esch, M., Mauritsen, T., Crueger, T., Rast, S., ... Roeckner, E. (2013). Atmospheric component of the MPI-M Earth System Model: ECHAM6. *Journal of Advances in Modeling Earth Systems*, *5*(2), 146-172. Retrieved from https://agupubs.onlinelibrary.wiley.com/doi/abs/10.1002/jame.20015 doi: 10.1002/jame.20015

Stouffer, R. (2019). *U of Arizona MCM-UA-1-0 model output prepared for CMIP6 CMIP.* Earth System Grid Federation. Retrieved from https://doi.org/10.22033/ESGF/CMIP6.2421 doi: 10.22033/ESGF/CMIP6.2421

Swart, N. C., Cole, J. N., Kharin, V. V., Lazare, M., Scinocca, J. F., Gillett, N. P., ... Sigmond, M. (2019). *CCCma CanESM5 model output prepared for CMIP6 CMIP.* Earth System Grid Federation. Retrieved from https://doi.org/10.22033/ESGF/CMIP6.1303 doi: 10.22033/ESGF/CMIP6.1303

Tang, Y., Rumbold, S., Ellis, R., Kelley, D., Mulcahy, J., Sellar, A., ... Jones, C. (2019). *MOHC UKESM1.0-LL model output prepared for CMIP6 CMIP.* Earth System Grid Federation. Retrieved from https://doi.org/10.22033/ESGF/CMIP6.1569 doi: 10.22033/ESGF/CMIP6.1569

Tatebe, H., & Watanabe, M. (2018). *MIROC MIROC6 model output prepared for CMIP6 CMIP.* Earth System Grid Federation. Retrieved from https://doi.org/10.22033/ESGF/CMIP6.881 doi: 10.22033/ESGF/CMIP6.881

Timmermann, A. (2001). Changes of enso stability due to greenhouse warming. *Geophysical Research Letters*, *28*(10), 2061-2064. Retrieved from https://agupubs.onlinelibrary.wiley.com/doi/abs/10.1029/2001GL012879 doi: https://doi.org/10.1029/2001GL012879

Timmermann, A., Oberhuber, J., Bacher, A., Esch, M., Latif, M., & Roeckner, E. (1999). Increased El Niño frequency in a climate model forced by future greenhouse warming. *Nature*, *398*, 694-697. Retrieved from https://doi.org/10.1038/19505 doi: 10.1038/19505

Voldoire, A. (2018). *CNRM-CERFACS CNRM-CM6-1 model output prepared for CMIP6 CMIP.* Earth System Grid Federation. Retrieved from https://doi.org/10.22033/ESGF/CMIP6.1375 doi: 10.22033/ESGF/CMIP6.1375

Voldoire, A. (2019). *CNRM-CERFACS CNRM-CM6-1-HR model output prepared for CMIP6 CMIP.* Earth System Grid Federation. Retrieved from https://doi.org/10.22033/ESGF/CMIP6.1385 doi: 10.22033/ESGF/CMIP6.1385

Volodin, E., Mortikov, E., Gritsun, A., Lykossov, V., Galin, V., Diansky, N., ... Emelina, S. (2019a). *INM INM-CM4-8 model output prepared for CMIP6 CMIP.* Earth System Grid Federation. Retrieved from https://doi.org/

10.22033/ESGF/CMIP6.1422 doi: 10.22033/ESGF/CMIP6.1422

Volodin, E., Mortikov, E., Gritsun, A., Lykossov, V., Galin, V., Diansky, N., ... Emelina, S. (2019b). *INM INM-CM5-0 model output prepared for CMIP6 CMIP.* Earth System Grid Federation. Retrieved from https://doi.org/10.22033/ESGF/CMIP6.1423 doi: 10.22033/ESGF/CMIP6.1423

Wang, G., Cai, W., Gan, B., Wu, L., Santoso, A., Lin, X., ... McPhaden, M. J. (2017). Continued increase of extreme El Niño frequency long after 1.5 °C warming stabilization. *Nature Climate Change*, *7*(8), 568-572. Retrieved from https://ui.adsabs.harvard.edu/abs/2017NatCC...7..568W doi: 10.1038/nclimate3351

Wieners, K.-H., Giorgetta, M., Jungclaus, J., Reick, C., Esch, M., Bittner, M., ... Roeckner, E. (2019). *MPI-M MPIESM1.2-LR model output prepared for CMIP6 CMIP.* Earth System Grid Federation. Retrieved from https://doi.org/10.22033/ESGF/CMIP6.742 doi: 10.22033/ESGF/CMIP6.742

Xin, X., Zhang, J., Zhang, F., Wu, T., Shi, X., Li, J., ... Wei, M. (2018). *BCC BCC-CSM2MR model output prepared for CMIP6 CMIP.* Earth System Grid Federation. Retrieved from https://doi.org/10.22033/ESGF/CMIP6.1725 doi: 10.22033/ESGF/CMIP6.1725

Xu, K., Tam, C.-Y., Zhu, C., Liu, B., & Wang, W. (2017). CMIP5 Projections of Two Types of El Niño and Their Related Tropical Precipitation in the Twenty-First Century. *Journal of Climate*, *30*(3), 849 - 864. Retrieved from https://journals.ametsoc.org/view/journals/clim/30/3/jcli-d-16-0413.1.xml doi: 10.1175/JCLI-D-16-0413.1

Yang, H., Zhang, Q., Zhong, Y., Vavrus, S., & Liu, Z. (2005). How does extratropical warming affect ENSO? *Geophysical Research Letters*, *32*(1). Retrieved from https://agupubs.onlinelibrary.wiley.com/doi/abs/10.1029/2004GL021624 doi: https://doi.org/10.1029/2004GL021624

Yukimoto, S., Koshiro, T., Kawai, H., Oshima, N., Yoshida, K., Urakawa, S., ... Adachi, Y. (2019). *MRI MRI-ESM2.0 model output prepared for CMIP6 CMIP.* Earth System Grid Federation. Retrieved from https://doi.org/10.22033/ESGF/CMIP6.621 doi: 10.22033/ESGF/CMIP6.621

Zelle, H., van Oldenborgh, G. J., Burgers, G., & Dijkstra, H. (2005). El Niño and Greenhouse Warming: Results from Ensemble Simulations with the NCAR CCSM. *Journal of Climate*, *18*(22), 4669 - 4683. Retrieved from https://journals.ametsoc.org/view/journals/clim/18/22/jcli3574.1.xml doi: 10.1175/JCLI3574.1

Zhang, J., Wu, T., Shi, X., Zhang, F., Li, J., Chu, M., ... Wei, M. (2018). *BCC BCC-ESM1 model output prepared for CMIP6 CMIP.* Earth System Grid Federation. Retrieved from https://doi.org/10.22033/ESGF/CMIP6.1734 doi: 10.22033/ESGF/CMIP6.1734

Zheng, X.-T., Hui, C., & Yeh, S.-W. (2018). Response of ENSO amplitude to global warming in CESM large ensemble: uncertainty due to internal variability. *Climate Dynamics*, *50*(11), 4019–4035. Retrieved from https://doi.org/10.1007/s00382-017-3859-7 doi: 10.1007/s00382-017-3859-7

Ziehn, T., Chamberlain, M., Lenton, A., Law, R., Bodman, R., Dix, M., ... Druken, K. (2019). *CSIRO ACCESS-ESM1.5 model output prepared for CMIP6 CMIP.* Earth System Grid Federation. Retrieved from https://doi.org/10.22033/ESGF/CMIP6.2288 doi: 10.22033/ESGF/CMIP6.2288